ACS OMEGA

Article

Cite This: ACS Omega 2018, 3, 6476−6482

Identification of Tobacco Types and Cigarette Brands Using an Electronic Nose Based on Conductive Polymer/Porphyrin Composite Sensors

C. Henrique A. Esteves,[†,⊥] Bernardo A. Iglesias,[†,∥] Takuji Ogawa,[‡] Koiti Araki,[†] Lucélia Hoehne,[§] and Jonas Gruber*[,†]

[†]Departamento de Química Fundamental, Instituto de Química, Universidade de São Paulo, Avenida Professor Lineu Prestes, 748, 05508-000 São Paulo, São Paulo, Brazil

[‡]Graduate School of Science, Department of Chemistry, Osaka University, Toyonaka, Osaka 560 0043, Japan

[§]Centro Universitário UNIVATES, Av. Avelino Talini 171, 95900-000 Lajeado, Rio Grande do Sul, Brazil

[∥]Departamento de Química, Universidade Federal de Santa Maria, Avenida Roraima, 1000, 97105-900 Santa Maria, Rio Grande do Sul, Brazil

Supporting Information

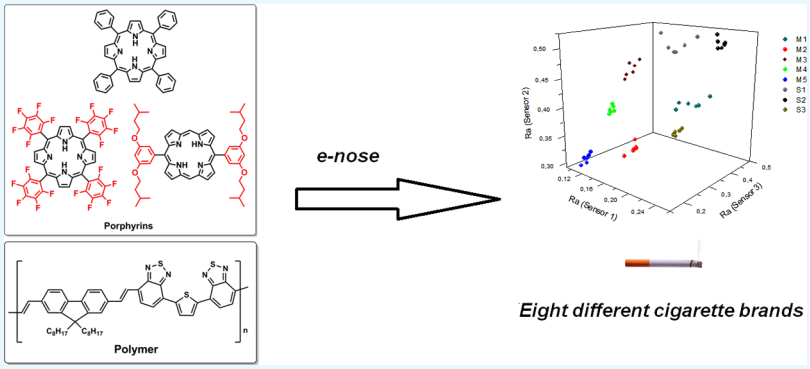

ABSTRACT: Three tobacco types (Burley, Flue Cured, and Oriental) and eight cigarette brands were unequivocally identified using an electronic nose formed by only three sensors based on a single novel conducting polymer (**PF-BTB**) doped with different porphyrins (**H_2TPP**, **H_2TPFP**, and **H_2BTBOP**). The synthesis and characterization of the polymer are also discussed. Small changes in the porphyrin structure caused significant changes in the electrical conductance response patterns of the sensors upon exposure to complex chemical matrixes, representing a novel approach for tuning the selectivity of chemiresistive sensors for e-nose application. This e-nose is fast, cheap, reliable, can be easily operated, and could be a valuable tool for border agents fighting cigarette smuggling around the world, helping them prevent losses of millions in tax revenues and sales.

1. INTRODUCTION

Fraudulent imitation of commercial products such as cigarettes is a problem worldwide. In Brazil, the cigarette industry and the government lose yearly millions in sales and tax revenue because of such illegal activity.[1] Usually, a visual inspection performed by a trained agent is not enough to identify counterfeiting, requiring an auxiliary analytical method to support an apprehension. In Brazil, the vast majority of counterfeit cigarettes enter the country via land borders and, because they are normally located in remote areas (frequently dense forests), a cheap, rapid, and portable system is necessary to help border agents in the task. Electronic noses (e-noses) come as a reasonable choice to meet all of these requirements.

e-Noses have been used to identify a great variety of analytes since their development in 1982.[2] This powerful tool has assisted many fields of knowledge, from medicine to chemistry, being applied in distinct situations, such as wine-quality inspection,[3] tuberculosis diagnosis,[4] characterization of juices,[5] and differentiation of aromatic flowers.[6] Food analysis is one of the most reported in literature,[7] and the reason for that lies on the fact that most products in this industry come from animal or vegetal sources, therefore containing a great variety of chemical compounds in their composition. This complexity challenges traditional analytical methods but, on the other hand, gives a perfect kind of matrix e-noses that are needed to perform a reliable differentiation.

e-Noses work with an array of sensors, each of them capable of changing its behavior differently when exposed to volatile substances released by analytes. These responses together produce a pattern that is sent to a single processing system and,

Received: March 5, 2018
Accepted: May 31, 2018
Published: June 18, 2018

DOI: 10.1021/acsomega.8b00403
ACS Omega 2018, 3, 6476−6482

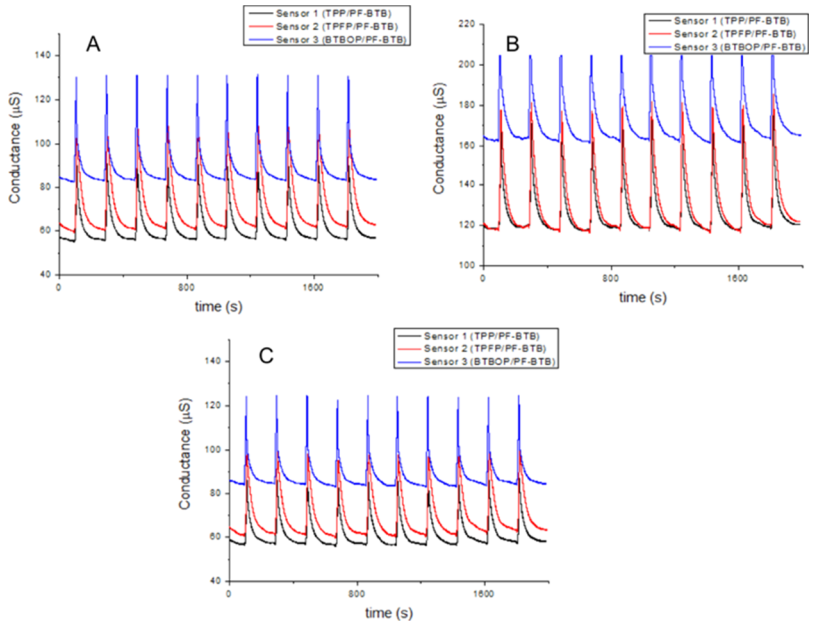

Figure 1. Conductance outputs. A: Burley; B: Flue Cured; and C: Oriental.

to provide a good identification, it must be unique to each of the analyzed aromas.[8] Sensors of different nature, relying on different chemical and physical phenomena, can play this role in the e-nose apparatus. Despite their different nature, they all aim at creating a pattern to identify the volatile compounds they are exposed to.[9] Among the most popular types are polymeric sensors, composed by a doped conductive polymer layer, which is capable of changing its conductivity when exposed to organic vapors.[10] Some advantages of this material are room-temperature operation, low power consumption, fast responses, high selectivity, and virtually unlimited possible polymeric structures.[11] The polymeric thin film deposited on the surface of these sensors interacts with the incoming vapors, which causes a conformational change in the structure. This phenomenon affects the conductivity observed and is specific to each type of matrix analyzed, forming the physical basis for the detection of compounds.[12] A further discussion of the detection mechanism has been previously published.[15]

Cigarette brand and tobacco analyses by e-noses have been reported in the literature using different sensors (e.g., metal oxide semiconductors and conductive polymer/carbon black)[13] and other techniques;[14] however, the complexity of these e-noses systems is higher when compared to the methodology discussed herein, employing 6 to 32 different sensors to perform these analyses. In a previous paper,[15] we first reported a new type of composite layer to be used in e-noses: a single conductive polymer had its chemiresistive behavior modulated by chemical interaction with different porphyrins, generating independent analytical signals and, therefore, producing a rich pattern for each analyte studied. As a proof of concept, an e-nose formed by these three sensors was used for classifying four volatile organic solvents (propanone, ethanol, ethyl acetate, and toluene). To further explore this idea and solve a real analytical problem, this work was focused on testing a far more complex system, tobaccos and cigarettes, analyzing the volatile compounds released by these samples. Also, a novel conductive polymer, **PF-BTB**, was synthesized, characterized, and employed for this task, showing the versatility of this active layer system.

2. RESULTS AND DISCUSSION

A three-sensor array was initially used to identify the three most common tobacco types produced in Brazil: Burley, Flue Cured, and Oriental. This experiment was planned to test the e-nose system and opened the possibility to more complex approaches, carried out afterward. The outputs registered in these experiments are shown in Figure 1.

The data were mathematically processed to calculate the relative response (R_a) parameter to each exposure/recovery cycle for each analyzed tobacco. The R_a parameter expresses the interaction between the sensor and the volatiles released by the analyte. G_1 and G_2 represent, respectively, the absolute conductance measured immediately before and after the exposure (Figure 2).

Calculated (R_a)s for the last six peaks in each graph, as shown in Figure 1, were plotted in a three-dimensional scatter (Figure 3), revealing three well-separated clusters that provided an outstanding classification.

On the basis of the good selectivity observed in Figure 3, the e-nose was subjected to a more complex test: screening eight

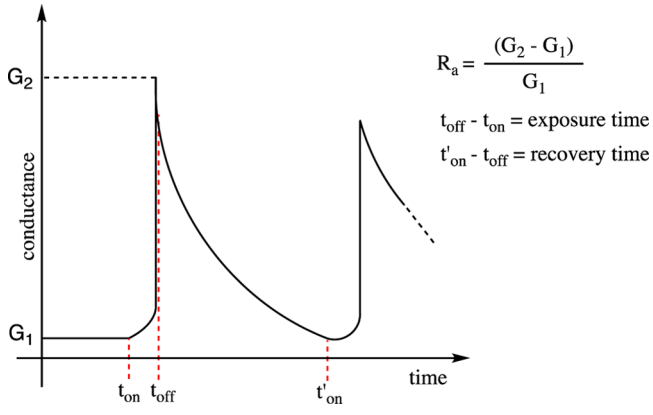

Figure 2. Response pattern and R_a calculation. t_{on} = V1 and V2 on and V3 off; t_{off} = V1 and V2 off and V3 on. For V1, V2, and V3, see Figure 11.

DOI: 10.1021/acsomega.8b00403
ACS Omega 2018, 3, 6476−6482

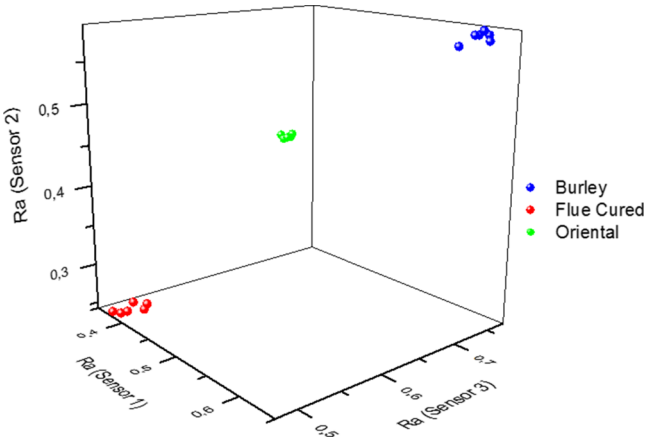

Figure 3. Plot of the relative responses (R_a)s for tobacco types.

different cigarette brands (Table 1) under the same conditions. Figure 4 shows two outputs as an example (one for each supplier; please see the supporting information for the complete set of conductance outputs).

Table 1. Cigarette Brands Tested and Their Attributed Codes

code	brand	supplier
M1	Marlboro Silver	Philip Morris
M2	Marlboro Gold	Philip Morris
M3	Marlboro	Philip Morris
M4	Marlboro Blue Ice	Philip Morris
M5	Marlboro Fresh Mint	Philip Morris
S1	Dunhill	Souza Cruz
S2	Lucky Strike	Souza Cruz
S3	Derby	Souza Cruz

Employing the same mathematical procedure described in Figure 2, a new three-dimensional scatter was plotted and, again, a very good clustering is observed, despite the number of brands analyzed (Figure 5).

3. CONCLUSIONS

The results presented in this work showed a very efficient e-nose based on composite sensors. The scope of its application was considerably expanded from simple compounds (organic solvents) to very complex chemical matrixes, presented herein. A new conductive polymer, **PF-BTB**, combined in pairs with

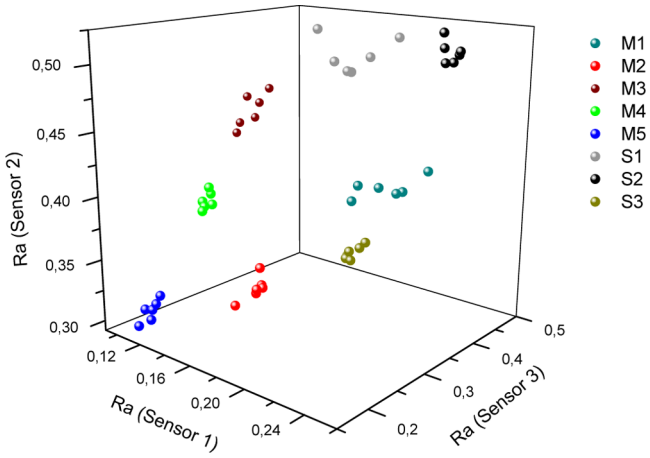

Figure 5. Plot of the relative responses (R_a)s for cigarette brands.

porphyrins **H2TPP**, **H2TPFP**, or **H2BTBOP**, generated three autonomous sensors and a fully functional e-nose array. The behavior of these pairs demonstrated their different nature, as only three distinct sensors would be capable of performing a very complicated identification involving eight chemically similar analytes (Figure 5). This result suggests an intimate molecular relationship between conductive polymers and porphyrins, showing that substitutions in these macrocyclic structures lead to substantial changes in the chemiresistive behavior of these pairs.

The analytical procedure proposed is fast, cheap, reliable and, above all, user friendly, which are all features essential to field applications carried out by border patrols fighting cigarette smuggling. The selectivity achieved broadens the application of this system to a great variety of brands and could make this method a valuable tool to differentiate genuine cigarettes from counterfeit products crossing every day national borders around the world.

4. MATERIALS AND METHODS

4.1. Solvents and Reagents. Commercial grade dimethylformamide (DMF; Aldrich) was dried over anhydrous $CuSO_4$ for 2 days and then distilled at 44−45 °C (25 mmHg) using a 40 cm Vigreux column and stored over freshly dried 4 Å molecular sieves.

Commercial grade chloroform (Synth) was heated under reflux over phosphorous pentoxide for 5 h, distilled at 58−60 °C (710 mmHg), and stored over freshly dried 4 Å molecular sieves.

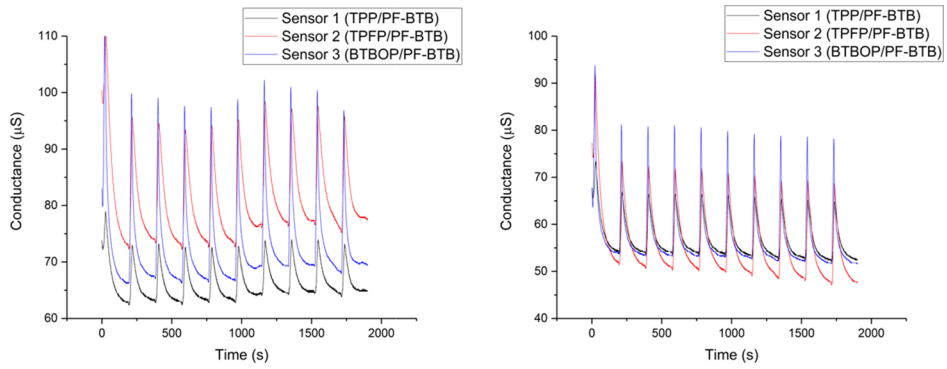

Figure 4. e-Nose outputs: Marlboro (left) and Lucky Strike (right).

DOI: 10.1021/acsomega.8b00403
ACS Omega 2018, 3, 6476−6482

Scheme 1. Synthetic Route toward PF-BTB

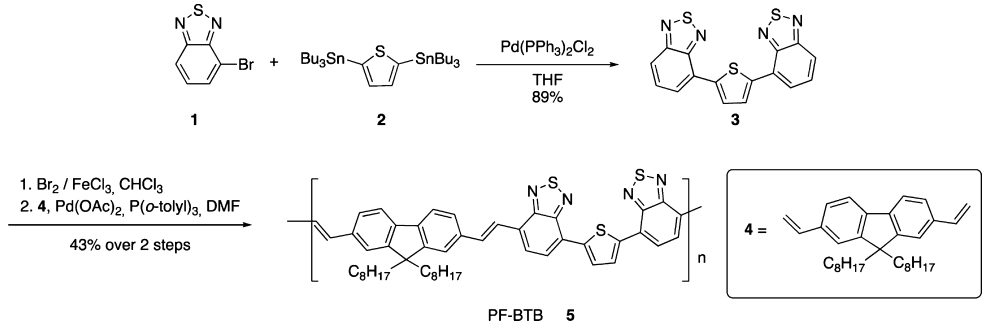

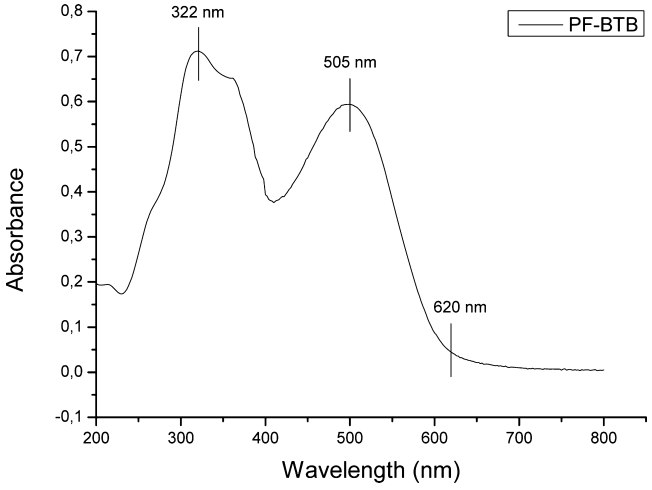

Figure 6. PF-BTB UV−vis absorption spectrum in chloroform solution.

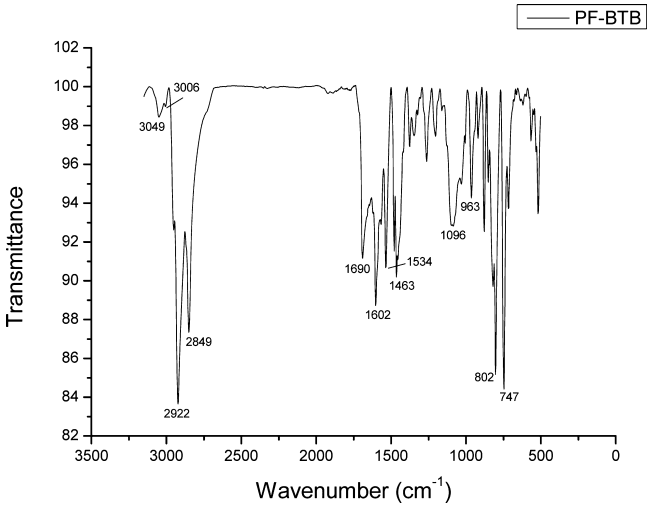

Figure 7. PF-BTB Infrared spectrum in KBr pellets.

Bromine (Aldrich) was shaken with concentrated H_2SO_4 1:1 (v/v) before use.

All other commercial chemicals were used as received (Aldrich).

4.2. Synthesis of PF-BTB. Poly(9,9-*n*-octyl-2,7-fluorenylenevinylene-*alt*-4,7-dibenzothiadiazole-2,5-thiophene), **PF-BTB** (**5**), was designed to be a low band gap polymer containing fluorene, thiophene, and 2,1,3-benzothiadiazole units, which have previously successfully produced low band gap polymers in similar structures.[16] The synthesis was carried out via Heck polymerization, following the synthetic pathway, as shown below (Scheme 1).

4-Bromo-2,1,3-benzothiadiazole (**1**),[17] 2,5-bis(tri-*n*-butylstannyl)thiophene (**2**),[18] and 9,9-dioctyl-2,7-divinyl-9*H*-fluorene (**4**) were synthesized according to literature procedures.[16b]

4.2.1. 2,5-Bis(benzo[c][1,2,5]thiadiazole-4-yl)thiophene (3). A solution containing 2,5-bis(tri-*n*-butylstannyl)thiophene (**2**) (1.44 g, 2.17 mmol), 4-bromo-2,1,3-benzothiadiazole 94%

Table 2. PF-BTB Infrared Bands Assignment[a]

experimental bands (cm^{-1})	literature data[17,21] (cm^{-1})	assignment
3049	3047	$\nu_{C-H\ aromatic}$ OP
3006	3024	$\nu_{C-H\ trans-vinyl}$ OP
2922	2920	$\nu_{aliphatic}$
2849	2852	$\nu_{aliphatic}$
1690	1679	$\nu_{C=N\ (benzothiadiazole)}$
1602	1594	$\nu_{C=C\ aromatic}$
1534	1561	$\nu_{C=C\ aromatic}$
1463	1423	$\nu_{C=C\ aromatic}$
1096	1108	$\delta_{C-H\ aromatic}$ IP
963	965	$\delta_{C-H\ trans-vinyl}$ IP
802	837	$\delta_{C-H\ aromatic}$ OP
747	784	unknown

[a]IP = in-plane, OP = out-of-plane.

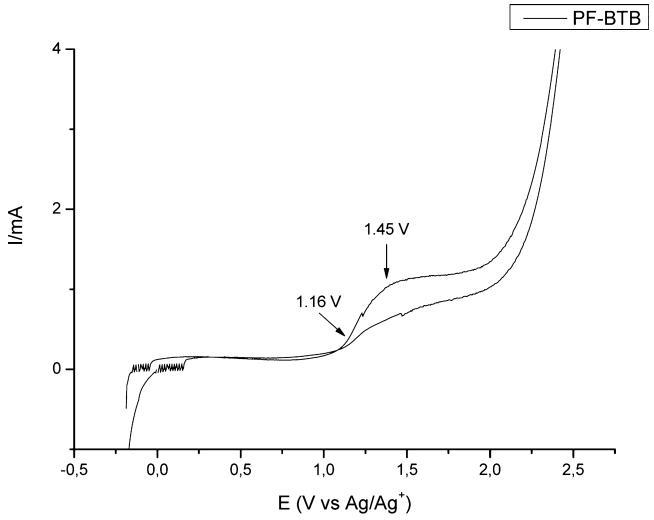

Figure 8. PF-BTB cyclic voltammetry in acetonitrile solution, using 0.2 M solution of $LiClO_4$ the as support electrolyte, at a scan rate of 50 mV/s.

DOI: 10.1021/acsomega.8b00403
ACS Omega 2018, 3, 6476−6482

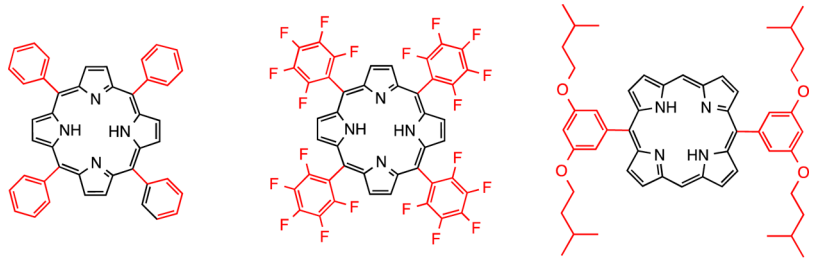

Figure 9. Synthesized porphyrins, H_2**TPP** (**6**), H_2**TPFP** (**7**), and H_2**BTBOP** (**8**).

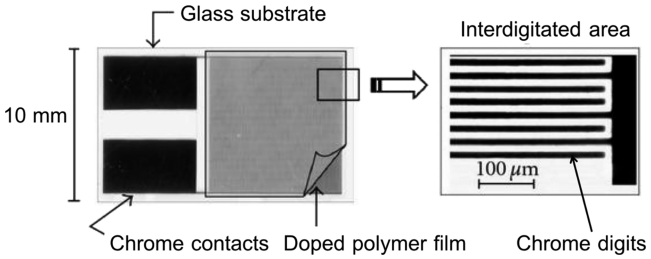

Figure 10. [25]Structure of the interdigitated sensor.

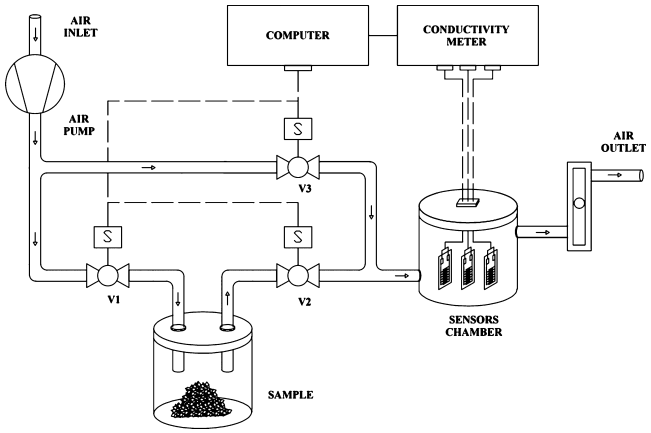

Figure 11. Schematic view of the e-nose measuring system.

(**1**) (1.00 g, 4.37 mmol), $PdCl_2(PPh_3)_2$ (0.03 g, 0.05 mmol), and anhydrous tetrahydrofuran (20 mL) was stirred under reflux for 5 h. The resulting mixture was washed with distilled water, and the aqueous phase was extracted three times with CH_2Cl_2. The organic phase was dried over $MgSO_4$ and evaporated under vacuum. The residue was purified by flash-column chromatography with (3:2 *n*-hexane/$CHCl_3$) as eluent to afford 0.680 g (1.92 mmol) of an orange solid (η = 88%). mp 180−183 °C (188−189 °C[19]).

^{1}H NMR (200 MHz, $CDCl_3$): δ 8.18 (s, 2H), 7.90−7.94 (m, 4H), 7.62 (t, J = 8.8 Hz, 2H).

^{13}C NMR (100 MHz, $CDCl_3$): δ 155.6, 152.2, 140.5, 129.7, 128.8, 127.4, 125.5, 120.4.

*4.2.2. Polymerization (**PF-BTB**) (**5**).* Br_2 (34 μL, 0.67 mmol) dissolved in $CHCl_3$ was added dropwise to a stirred solution of 2,5-bis(benzo[*c*][1,2,5]thiadiazole-4-yl)thiophene (**3**) (0.10 g, 0.28 mmol), $FeCl_3$ (0.90 mg, 5.6 μmol), and $CHCl_3$ (10 mL). The mixture was refluxed for 5 h, forming the brominated monomer BTB as an insoluble orange solid that was filtrated, washed with distilled water, and dried under vacuum overnight [^{1}H NMR (200 MHz, $CDCl_3$): δ 8.17 (s, 2H), 7.90 (d, J = 7.6 Hz, 2H), 7.79 (d, J = 7.6 Hz, 2H)]. Then, (0.10 g, 0.19 mmol) of this product was added without further purification to a reaction vessel containing 9,9-dioctyl-2,7-divinyl-9*H*-fluorene (**4**) (0.08 g, 0.19 mmol), P(*o*-tol)$_3$ (0.03 g, 0.10 mmol), $Pd(OAc)_2$ (3.8 mg, 0.02 mmol), triethylamine (1 mL), and 8 mL of anhydrous DMF. The mixture was degassed with anhydrous N_2 and heated to 90 °C for 48 h. The polymer was precipitated by adding 80 mL of methanol, filtrated, and dried under vacuum. The solid was washed, in sequence, with methanol and hexane for 1 h each using a Soxhlet apparatus. The liquids were discarded, and then the resulting solid was extracted thoroughly with chloroform during 24 h. The chloroform was evaporated affording 0.09 g of a black solid (η = 43% over two steps). Gel permeation chromatography analysis using polystyrene as the standard revealed that the weight-average molecular weight for **PF-BTB** is 2.9 kDa.

4.3. Characterization of PF-BTB. The polymer was initially characterized by UV−vis spectroscopy using a dilute chloroform solution (6 mg/L) (Figure 6).

The absorption spectrum shows two strong bands: the first one at 250−400 nm, representing $\pi_{\text{delocalized}}-\pi^*_{\text{localized}}$ and $\pi_{\text{localized}}-\pi^*_{\text{delocalized}}$ transitions, and the second one in the 425−620 nm range, representing $\pi-\pi^*$ transitions for π electron states delocalized along the polymer chain.[20] The polymer optical band gap (E_g) estimated from the absorption edge is 2.0 eV (620 nm).

The infrared spectrum was registered using KBr pellets and is shown in Figure 7. The tentative assignment of the most significant bands is listed in Table 2.

The bands at 963 and 3006 cm^{-1} reveal that the Heck polymerization formed trans-double bonds between the two monomeric units in **PF-BTB**.

A **PF-BTB** sample was casted onto an indium tin oxide-coated glass electrode which was used as the working electrode in a cyclic voltammetry experiment performed in a 0.2 M solution of $LiClO_4$ in acetonitrile at a scan rate of 50 mV/s, from −0.2 to 2.5 V, using a Pt wire as the counter electrode and Ag/Ag^+ as the reference electrode. Figure 8 shows a well-defined oxidation peak starting at 1.16 V [highest occupied molecular orbital (HOMO) energy] with a maximum at 1.45 V. Using the optical band gap, the reduction potential can be estimated at −0.84 V [lowest unoccupied molecular orbital (LUMO) energy].

4.4. Porphyrins Syntheses. *meso*-Tetra(phenyl)porphyrin (H_2**TPP**) (**6**),[22] *meso*-tetra(2,3,4,5,6-pentafluorophenyl)-porphyrin (H_2**TPFP**) (**7**),[23] and 5,15-({3,5-bis(isopentyloxy)-benzene}porphyrin) (H_2**BTBOP**) (**8**)[24] (Figure 9) were synthesized according to literature procedures.

4.5. Sensors Preparation. Stock solutions containing 2.5 mg of **PF-BTB**, 0.72 μmol of each free-base porphyrin (H_2**TPP**, H_2**BTBOP**, or H_2**TPFP**), and 0.75 mL of chloroform

DOI: 10.1021/acsomega.8b00403
ACS Omega 2018, 3, 6476−6482

were prepared. These solutions (20 μL) were deposited by spin-coating onto interdigitated electrodes (1 cm^2, 18 μm gap between digits),[16c,25] generating polymeric films of ≈1 μm thickness (Figure 10). The sensors were used over 1 week, showing no signs of decomposition or significant decrease in the conductivity observed.

4.6. e-Nose Apparatus. The e-nose system for dynamic sampling used in this work was entirely built in our laboratory and is shown, as a schematic representation, in Figure 11. A complete measure cycle is composed by an exposure phase (valves 1 and 2 open and valve 3 closed), when the sample headspace is carried to the sensors' chamber, and a recovery phase (valves 1 and 2 closed and valve 3 open), when ambient air passes through the sensors. Each analyte was kept in the sample compartment at 30 °C during the whole experiment, and the airflow was maintained at 0.6 $L \cdot min^{-1}$. For all analytes, the exposure (10 s)/recovery (180 s) cycle was repeated 10 times, and the four initial peaks were disconsidered. The conductance was registered by a conductivity meter,[26] operating with 80 mV peak-to-peak 2 kHz triangle wave ac voltage, and connected via a 10-bit analog-to-digital converter to a personal computer. The sensors do not require any type of cleaning or preparation between samples.

4.7. Sample Preparation. Burley, Flue Cured, and Oriental tobacco leaves, subjected to the same postharvest processing, were obtained from a national producer from Vale do Rio Pardo region, state of Rio Grande do Sul, Brazil, and grinded until the resulting aspect matched the tobacco found in cigarettes. All cigarettes were obtained from local suppliers, and the tobacco contained in a single cigarette was removed and placed in the sample's container for each measurement.

■ ASSOCIATED CONTENT

Supporting Information

The Supporting Information is available free of charge on the ACS Publications website at DOI: 10.1021/acsomega.8b00403.

Conductance versus time for all of the cigarette brands tested (PDF)

■ AUTHOR INFORMATION

Corresponding Author

*E-mail: jogruber@iq.usp.br. Phone: +55 11 3091-1103 (J.G.).

ORCID

Jonas Gruber: 0000-0003-2832-0199

Present Address

⊥Departamento de Farmácia, Faculdade de Ciências Farmacêuticas, Universidade de São Paulo, 05508-000 São Paulo, SP, Brazil.

Notes

The authors declare no competing financial interest.

■ ACKNOWLEDGMENTS

The authors thank Conselho Nacional de Desenvolvimento Científico e Tecnológico (CNPq) (443625/2014-0, 132622/2011-4, 303717/2010-6, and 307915/2013-1) and Fundação de Amparo à Pesquisa do Estado de São Paulo (FAPESP) (2011/51249-3) for their financial support; Dr. Gustavo P. Rehder and Prof. Marcelo N. P. Carreño for the interdigitated electrodes; and Daniel Kuhn, Eduardo M. Ethur, and Taciélen Altmayer for the tobacco samples.

■ REFERENCES

(1) Brazilian Federal Police, 2008; Annual Report.

(2) Persaud, K.; Dodd, G. Analysis of discrimination mechanisms in the mammalian olfactory system using a model nose. *Nature* **1982**, *299*, 352−355.

(3) (a) Macías, M. M.; Manso, A. G.; Orellana, C. J. G.; Velasco, H. M. G.; Caballero, R. G.; Chamizo, J. C. P. Acetic Acid Detection Threshold in Synthetic Wine Samples of a Portable Electronic Nose. *Sensors* **2013**, *13*, 208−220. (b) Berna, A. Z.; Trowell, S.; Cynkar, W.; Cozzolino, D. Comparison of metal oxide-based electronic nose and mass spectrometry-based electronic nose for the prediction of red wine spoilage. *J. Agric. Food Chem.* **2008**, *56*, 3238−3244.

(4) Bruins, M.; Rahim, Z.; Bos, A.; van de Sande, W. W. J.; Endtz, H. P.; van Belkum, A. Diagnosis of active tuberculosis by e-nose analysis of exhaled air. *Tuberculosis* **2013**, *93*, 232−238.

(5) Qiu, S.; Wang, J.; Gao, L. Discrimination and Characterization of Strawberry Juice Based on Electronic Nose and Tongue: Comparison of Different Juice Processing Approaches by LDA, PLSR, RF, and SVM. *J. Agric. Food Chem.* **2014**, *62*, 6426−6434.

(6) Wali, R. P. An electronic nose to differentiate aromatic flowers using a real-time information-rich piezoelectric resonance measurement. *Procedia Chem.* **2012**, *6*, 194−202.

(7) (a) Loutfi, A.; Coradeschi, S.; Mani, G. K.; Shankar, P.; Rayappan, J. B. B. Electronic noses for food quality: a review. *J. Food Eng.* **2015**, *144*, 103−111. (b) Severini, C.; Ricci, I.; Marone, M.; Derossi, A.; De Pilli, T. Changes in the Aromatic Profile of Espresso Coffee as a Function of the Grinding Grade and Extraction Time: A Study by the Electronic Nose System. *J. Agric. Food Chem.* **2015**, *63*, 2321−2327. (c) Rizzolo, A.; Bianchi, G.; Vanoli, M.; Lurie, S.; Spinelli, L.; Torricelli, A. Electronic Nose to Detect Volatile Compound Profile and Quality Changes in 'Spring Belle' Peach (*Prunus persica* L.) during Cold Storage in Relation to Fruit Optical Properties Measured by Time-Resolved Reflectance Spectroscopy. *J. Agric. Food Chem.* **2013**, *61*, 1671−1685. (d) Arroyo, T.; Lozano, J.; Cabellos, J. M.; Gil-Diaz, M.; Santos, J. P.; Horrillo, C. Evaluation of Wine Aromatic Compounds by a Sensory Human Panel and an Electronic Nose. *J. Agric. Food Chem.* **2009**, *57*, 11543−11549. (e) Echeverría, G.; Correa, E.; Ruiz-Altisent, M.; Graell, J.; Puy, J.; Lopez, L. Characterization of Fuji Apples from Different Harvest Dates and Storage Conditions from Measurements of Volatiles by Gas Chromatography and Electronic Nose. *J. Agric. Food Chem.* **2004**, *52*, 4582.

(8) Smyth, H.; Cozzolino, D. Instrumental Methods (Spectroscopy, Electronic Nose, and Tongue) As Tools to Predict Taste and Aroma in Beverages: Advantages and Limitations. *Chem. Rev.* **2013**, *113*, 1429−1440.

(9) Falasconi, M.; Concina, I.; Gobbi, E.; Sberveglieri, V.; Pulvirenti, A.; Sberveglieri, G. Electronic Nose for Microbiological Quality Control of Food Products. *Int. J. Electrochem.* **2012**, *2012*, 715763.

(10) James, D.; Scott, S. M.; Ali, Z.; O'Hare, W. T. Chemical Sensors for Electronic Nose Systems. *Microchim. Acta* **2005**, *149*, 1−17.

(11) Péres, L. O.; Gruber, J. The use of block copolymers containing PPV in gas sensors for electronic noses. *Mater. Sci. Eng., C* **2007**, *27*, 67−69.

(12) Caseli, L.; Gruber, J.; Li, R. W. C.; Péres, L. O. Investigation of the Conformational Changes of a Conducting Polymer in Gas Sensor Active Layers by Means of Polarization-Modulation Infrared Reflection Absorption Spectroscopy (PM-IRRAS). *Langmuir* **2013**, *29*, 2640−2645.

(13) (a) Luo, D.; Hosseini, H. G.; Stewart, J. R. Application of ANN with extracted parameters from an electronic nose in cigarette brand identification. *Sens. Actuators, B* **2004**, *99*, 253−257. (b) Brudzewski, K.; Osowski, S.; Golembiecka, A. Differential electronic nose and support vector machine for fast recognition of tobacco. *Expert Syst. Appl.* **2012**, *39*, 9886−9891. (c) Haddi, Z.; Amari, A.; Alami, H.; El Bari, N.; Llobet, E.; Bouchikhi, B. A portable electronic nose system for the identification of cannabis-based drugs. *Sens. Actuators, B* **2011**, *155*, 456−463. (d) Brudzewski, K.; Osowski, S.; Ulaczyk, J. Differential electronic nose of two chemo sensor arrays for odor discrimination. *Sens. Actuators, B* **2010**, *145*, 246−249.

DOI: 10.1021/acsomega.8b00403
ACS Omega 2018, 3, 6476−6482

(14) (a) Zook, C. M.; Patel, P. M.; LaCourse, W. R.; Ralapati, S. Characterization of Tobacco Products by High-Performance Anion Exchange Chromatography−Pulsed Amperometric Detection. *J. Agric. Food Chem.* **1996**, *44*, 1773−1779. (b) Ng, L.-K.; Lafontaine, P.; Vanier, M. Characterization of Cigarette Tobacco by Direct Electrospray Ionization−Ion Trap Mass Spectrometry (ESI-ITMS) Analysis of the Aqueous Extract: A Novel and Simple Approach. *J. Agric. Food Chem.* **2004**, *52*, 7251−7257. (c) Zhang, L.; Wang, X.; Guo, J.; Xia, Q.; Zhao, G.; Zhou, H.; Xie, F. Metabolic Profiling of Chinese Tobacco Leaf of Different Geographical Origins by GC-MS. *J. Agric. Food Chem.* **2013**, *61*, 2597−2605. (d) Xia, B.; Feng, M.; Xu, G.; Xu, J.; Li, S.; Chen, X.; Ding, L.; Zhou, Y. Investigation of the Chemical Compositions in Tobacco of Different Origins and Maturities at Harvest by GC−MS and HPLC−PDA-QTOF-MS. *J. Agric. Food Chem.* **2014**, *62*, 4979−4987.

(15) Esteves, C. H. A.; Iglesias, B. A.; Li, R. W. C.; Ogawa, T.; Araki, K.; Gruber, J. Identification of organic solvents using a new composite porphyrin-conductive polymer gas sensor. *Sens. Actuators, B* **2013**, *193*, 136−141.

(16) (a) Xu, S.; Liu, Y.; Li, J.; Wang, Y.; Cao, S. Synthesis and characterization of low-band-gap conjugated polymers containing phenothiazine and benzo-2,1,3-thia-/seleno-diazole. *Polym. Adv. Technol.* **2010**, *21*, 663−668. (b) Pei, J.; Wen, S.; Zhou, Y.; Dong, Q.; Liu, Z.; Zhang, J.; Tian, W. A low band gap donor-acceptor copolymer containing fluorene and benzothiadiazole units: synthesis and photovoltaic properties. *New J. Chem.* **2011**, *35*, 385−393. (c) Cordeiro, J. R.; Li, R. W. C.; Takahashi, E. S.; Rehder, G. P.; Ceccantini, G.; Gruber, J. Wood identification by a portable low-cost polymer-based electronic nose. *RSC Adv.* **2016**, *6*, 109945−109949. (d) Bundgard, E.; Krebs, F. C. Low-Band-Gap Conjugated Polymers Based on Thiophene, Benzothiadiazole, and Benzobis(thiadiazole). *Macromolecules* **2006**, *39*, 2823−2831.

(17) Pilgram, K.; Zupan, M.; Skiles, R. Bromination of 2,1,3-Benzotiadiazoles. *J. Heterocycl. Chem.* **1970**, *3*, 629−633.

(18) Wei, Y.; Yang, Y.; Yeh, J.-M. Synthesis and Electronic Properties of Aldehyde End-capped Thiophene Oligomers and Other α,ω-Substituted Sexthiophene. *Chem. Mater.* **1996**, *8*, 2659−2666.

(19) Zimdars, S.; Langhals, H.; Knochel, P. Functionalization of the [c][1,2,5]thiazole Scafold via Mg-, Zn- and Mn-Intermediates. *Synthesis* **2011**, *8*, 1302−1308.

(20) Bradley, D. D. C. Precursor-route poly(*p*-phenylenevinylene): polymer characterization and control of electronic properties. *J. Phys. D: Appl. Phys.* **1987**, *20*, 1389−1410.

(21) Mancilha, F. S.; Neto, B. A. D.; Lopes, A. S.; Moreira, P. F., Jr.; Quina, F. H.; Gonçalves, R. S.; Dupont, J. Are Molecular 5,8-π-Extended Quinoxaline Derivatives Good Chromophores for Photoluminescence Applications. *Eur. J. Org. Chem.* **2006**, 4924−4933.

(22) Lindsey, J. S.; Schreiman, I. C.; Hsu, H. C.; Kearney, P. C.; Marguerettaz, A. M. Rothemund and Adler-Longo Reactions Revisited: Synthesis of Tetraphenylporphyrins under Equilibrium Conditions. *J. Org. Chem.* **1987**, *52*, 827−836.

(23) Chen, X.; Hui, L.; Foster, D. A.; Drain, C. M. Efficient synthesis and photodynamic activity of porphyrin-saccharide conjugates: targeting and incapacitating cancer cells. *Biochemistry* **2004**, *43*, 10918−10929.

(24) Littler, B. J.; Ciringh, Y.; Lindsey, J. S. Investigation of conditions giving minimal scrambling in the synthesis of trans-porphyrins from dipyrromethanes and aldehydes. *J. Org. Chem.* **1999**, *64*, 2864−2872.

(25) Cordeiro, J. R.; Martinez, M. I. V.; Li, R. W. C.; Cardoso, A. P.; Nunes, L. C.; Krug, F. J.; Paixão, T. R. L. C.; Nomura, C. S.; Gruber, J. Identification of four wood species by an electronic nose and by LIBS. *Int. J. Electrochem.* **2012**, *2012*, 563939.

(26) da Rocha, R. T.; Gutz, L. G. R.; do Lago, C. A low-cost and high-performance conductivity meter. *J. Chem. Educ.* **1997**, *74*, 572−574.

DOI: 10.1021/acsomega.8b00403
ACS Omega 2018, 3, 6476−6482